PHYSICAL REVIEW A **73**, 041407(R) (2006)

Electrodynamically trapped Yb^+ ions for quantum information processing

Chr. Balzer,[1] A. Braun,[1] T. Hannemann,[1] Chr. Paape,[2] M. Ettler,[2] W. Neuhauser,[2] and Chr. Wunderlich[1]
[1]*Fachbereich Physik, Universität Siegen, 57068 Siegen, Germany*
[2]*Institut für Laser-Physik, Universität Hamburg, Luruper Chaussee 149, 22761 Hamburg, Germany*
(Received 3 February 2006; published 28 April 2006)

Highly efficient, nearly deterministic, and isotope selective generation of Yb^+ ions by one- and two-color photoionization is demonstrated. State preparation and state selective detection of hyperfine states in $^{171}Yb^+$ is investigated in order to optimize the purity of the prepared state and to time-optimize the detection process. Linear laser-cooled Yb^+ ion crystals confined in a Paul trap are demonstrated. Advantageous features of different previous ion trap experiments are combined, while at the same time the number of possible error sources is reduced by using a comparatively simple experimental apparatus. This opens a new path toward quantum state manipulation of individual trapped ions, and in particular, to scalable quantum computing.

DOI: 10.1103/PhysRevA.73.041407 PACS number(s): 32.80.Pj, 03.67.Lx, 32.80.Fb

When investigating fundamental questions related to quantum mechanics, experiments are called for where individual quantum systems can be accessed and deterministically manipulated. The interaction of trapped atomic ions among themselves and with their environment can be controlled to a high degree of accuracy, and thus allows for the preparation of well-defined quantum states of the ions' internal and motional degrees of freedom. Trapped ions have proven to be well suited for a multitude of investigations, for instance, into entanglement, decoherence, and quantum information processing, and for applications such as atomic frequency standards. Quantum information processing, in particular, requires the accurate and precise control of internal and often of motional quantum dynamics of a collection of trapped ions. In order to eliminate sources of possible errors, and thus prepare the ground to attain the ambitious goal of using trapped ions for large-scale quantum computing or quantum simulations, it is desirable to simplify the apparatus used for such experiments as far as possible.

An unprecedented degree of control of quantum systems has been reached in recent experiments with trapped ions, for instance, with Be^+ [1], Ca^+ [2], and Cd^+ [3] ions. Mainly the type of ion used in such experiments determines the experimental infrastructure needed for the controlled manipulation of these ions. The available ionic transitions, for instance, determine the radiation sources to be used: In Ca^+, an optical electric quadrupole transition has been used as a qubit leading to a coherence time ultimately limited by spontaneous radiative decay. More importantly, phase fluctuations of the laser light driving the qubit transition limit the available coherence time, even when using a highly sophisticated light source [5]. Phase fluctuations of the radiation driving the qubit transition do not present a major obstacle, if a hyperfine transition is used as a qubit (as, for instance, in Be^+ or Cd^+), since such a transition is usually excited by a stimulated two-photon Raman process where only relative fluctuations between the two driving fields limit the available coherence time. Choosing magnetic field insensitive states as a qubit, as was demonstrated recently with Yb^+ [4] and Be^+ [6], may further contribute to achieving the desired long coherence times.

Another important characteristic that determines the suitability of a particular ion for experiments requiring quantum dynamics with minimal error is the initial preparation in one of the qubit states (before coherent operations take place), and state selective detection. This usually makes additional light fields necessary, such that up to a total of seven different light sources are in use in some experiments [7].

For laser cooling of trapped ions, a suitable optical electric dipole transition is usually used. In Ca^+, the required wavelengths are accessible by diode lasers as opposed to Be^+ and Cd^+ where the necessary wavelengths are in the deep UV region, making more complex laser systems and nonstandard optical elements necessary.

The efficient production of singly charged ions by photoionization of its neutral precursor was recently demonstrated with Ca^+ [7,8]. This way of producing ions avoids difficulties that arise when employing ionization by electron collision as done in experiments, for instance, with Be^+ and, at the same time, allows for isotope selective loading of ion traps.

Spectroscopic studies of Yb^+ ions have been carried out in order to use single ions or an ensemble of these ions to implement improved frequency standards [9]. In this paper, we report on experiments with electrodynamically trapped Yb^+ ions where advantageous features of previous experiments with trapped Ca^+, Be^+, and Cd^+ ions are combined: (i) Only two light fields, easily generated by standard laser sources, are needed for laser cooling and fluorescence detection [4]. (ii) Isotope selective photoionization of Yb and nearly deterministic loading of Yb^+ ions one by one into a linear electrodynamic trap is demonstrated. Highly efficient photoionization is achieved using just one additional light field delivered by a readily available diode laser. (iii) Laser-cooled linear crystals of individually resolved Yb^+ ions are formed in an electrodynamic trap, to our knowledge, for the first time. A laser-cooled Yb^+ ion crystal will be useful not only for QIP, but also to enhance the precision of a frequency standard based on ionic microwave transitions [10]. (iv) Two hyperfine states may serve as a qubit in $^{171}Yb^+$, thus essentially eliminating spontaneous decay. Using an optical Raman transition or microwave radiation [11] to drive a hyperfine transition allows for the extension of the coherence time even far beyond a second [4,6]. (v) Investigations of state

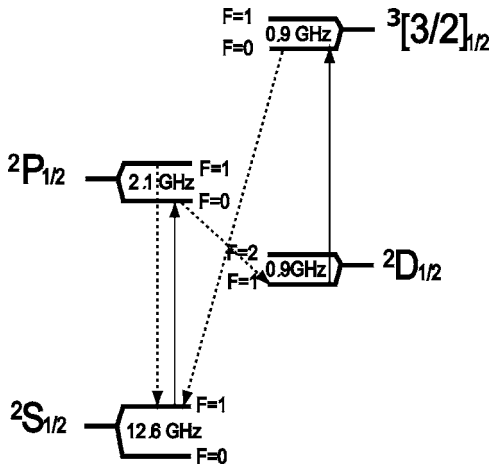

FIG. 1. Relevant energy levels and transitions of Yb^+ including the hyperfine splitting in $^{171}Yb^+$ (drawing is not to scale). The $S_{1/2}-P_{1/2}$ transition wavelength is 369 nm, and for $D_{3/2}-[3/2]_{1/2}$, it is 935 nm.

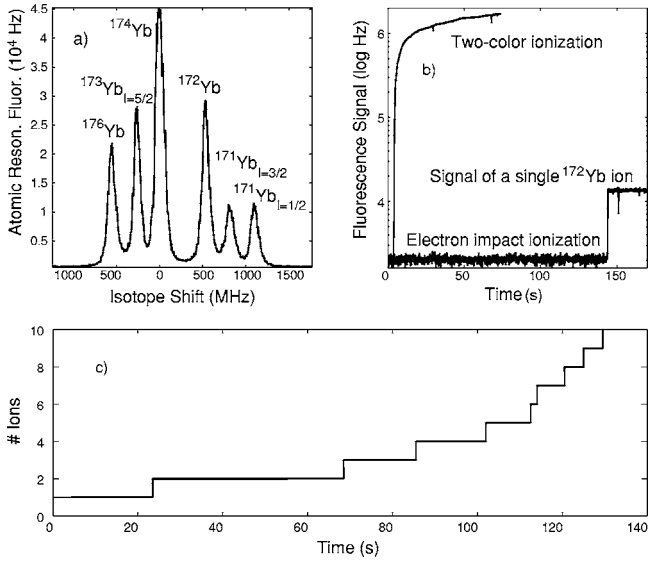

FIG. 2. (a) Isotope selective excitation of the $6s_2\ ^1S_0 \rightarrow 6s6p\ ^1P_1$ resonance in Yb (natural abundance). (b) Comparison of the trap loading rate using electron impact or photoionization. (c) Number of trapped $^{172}Yb^+$ ions as a function of time demonstrating the possibility of nearly deterministic loading of ions.

preparation and state selective detection are reported and these two processes are nearly optimized.

An electrodynamic Paul trap with four parallel rod electrodes (diameter of 0.5 mm) in a linear quadrupole configuration (inner radius of 0.75 mm) is used for the rf confinement of Yb^+ ion crystals in the radial direction [12]. Axial confinement is achieved by applying a dc voltage to two endcap electrodes (diameter of 0.4 mm) spaced 4 mm apart on axis, centered between the four rod electrodes. All electrodes are made of molybdenum and are held in place by ceramic spacers. The trap is operated at 21.6 MHz with a rf amplitude of approximately 400 V, resulting in radial secular frequencies of 350–450 kHz and an axial secular frequency of 40–60 kHz. Alternatively, a rf drive at 10.2 MHz is in use yielding radial and axial secular frequencies of 800 and 65 kHz, respectively. The endcap voltage is typically kept at about 1.0 V, in contrast to other linear traps, which report endcap voltages up to several hundred volts.

For some experiments on state preparation, a miniature Paul trap was used consisting of a ring electrode of diameter 2 mm and two endcap electrodes spaced $\approx\sqrt{2}$ nm apart (for more details on this trap, see [13]).

For each of the traps a photomultiplier is used to detect resonance fluorescence. In addition, an image intensified CCD (ICCD) camera is employed to spatially resolve the detected fluorescence. Imaging onto the ICCD camera is realized with a Questar long-distance microscope, thus ensuring minimal aberrations and yielding a magnification of about 30.

Figure 1 depicts relevant energy levels for Yb^+ ions. The electric dipole transition between the $S_{1/2}$ ground state and the $P_{1/2}$ excited state (natural linewidth of 19.6 MHz) serves for Doppler cooling, state preparation, and state selective detection (described below). This transition is driven using laser light with a wavelength near 369 nm generated by frequency doubling the output of a commercial Ti:sapphire laser. Optical pumping into the $D_{3/2}$ state is avoided by employing a diode laser-emitting light near 935 nm. The polarization of the light fields is at 45° with respect to the external magnetic field in order to couple all Zeeman sublevels to the cooling cycle. The $^{171}Yb^+$ isotope has a nuclear angular momentum $I=1/2$ that leads to the hyperfine splitting of all levels.

Several advantages make photoionization the preferred choice to load single ions into an ion trap. First, it avoids the charging up of electrically isolating elements near the trap center as with electron impact ionization. Second, due to its high efficiency and well-defined interaction volume, it allows for a reduction of the atom flux by several orders of magnitude, thereby minimizing contamination of the trap electrodes by neutral atoms. Both effects would lead to a disturbance of the trapping potential. Additionally, photoionization is an isotope-selective process, which is advantageous if the isotope-selected material is not available, or if one seeks to trap an isotope of low abundance.

A diode laser delivering light near 399 nm with an intensity of typically 3 W/cm^2 is employed to resonantly excite the transition between the ground state $6s_2\ ^1S_0$ and the excited state $6s6p\ ^1P_1$ in neutral Yb. This one-photon process is isotope selective. The absorption of a second photon near 369 nm (the wavelength used to drive the $S_{1/2} \leftrightarrow P_{1/2}$ transition in Yb^+) leads to ionization (two-color ionization). Alternatively, the second step of this ionization process is achieved by the absorption of another photon near 399 nm (one-color ionization). This is possible, since in the presence of the quasistatic electric trapping field, the ionization threshold is lowered. Both photoionization schemes yield ionization rates in the experiments reported that are 2 (one-color) or 3 (two-color) orders of magnitude larger than ionization by electron collision (keeping the same neutral atom flux), are isotope selective, and allow for nearly deterministic loading of ion traps.

Figure 2 depicts important features of the photoionization process. The collected resonance fluorescence as a function

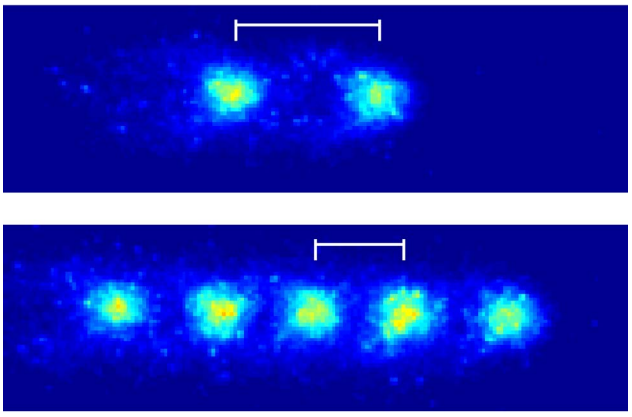

FIG. 3. (Color online) Spatially resolved detection of resonance fluorescence near 369 nm of a laser-cooled crystal of two and five $^{172}Yb^+$ ions, respectively. The length scales correspond to 26(2) μm (top) and 16(2) μm (bottom).

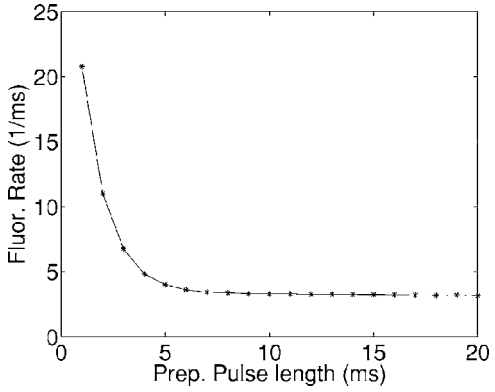

FIG. 4. Detected resonance fluorescence near 369 nm from a collection of ions as a function of time. The decrease with time indicates optical pumping into state $|0\rangle \equiv |S_{1/2}, F=0\rangle$. This optical pumping process serves for state readout and initialization (see text).

of the wavelength of the laser light exciting the atomic $6s_2\ ^1S_0 \leftrightarrow 6s6p\ ^1P_1$ transition is shown in Fig. 2(a). In order to reduce Doppler broadening, the atomic beam and the laser beam are set at a relative angle of 90°, thus allowing resolution of the isotopes with mass 171, 172, 173, 174, and 176 (in amu). Figure 2(b) compares the loading rates for electron impact and photoionization. It shows the total fluorescence signal as a function of time, while the trap is being loaded. During the time it takes to load a single ion using electron impact ionization, the trap has already been loaded using photoionization such that the fluorescence signal saturates (due to the limited acceptance angle of the optical elements). The rate for the electron impact ionization is of the order $1/150 \approx 0.0067$ ions/s, while with photoionization loading rates about 3 orders of magnitude larger, approximately 10 ions/s, are achieved. Finally, in Fig. 2(c) the atom flux is reduced such that the nearly deterministic loading of a desired number of ions becomes possible (during the course of the measurement, the Yb oven was heating up, thus leading to an increase of the loading rate with time). The exact number of ions in the trap is determined by counting them on the spatially resolved fluorescence image of the ICCD camera. The loading process can be interrupted at any time by blocking the ionization laser.

Figure 3 shows two spatially resolved images of resonance fluorescence near 369 nm scattered by a Doppler-cooled crystal of two or five $^{172}Yb^+$ ions, respectively (with the fluorescence intensity color coded). The images are averaged over 10 frames, with an illumination time of 200 ms for each frame. These images were recorded with an axial secular frequency $\omega_z = 2\pi \times 52$ kHz.

A quantum logic operation consists of three steps: first, the qubit is initialized in a given state. Second, qubit states are coherently manipulated, and third, the resulting state is measured. In the paragraphs to follow, the first and third steps for the case of the $^{171}Yb^+$ ion are described. The ability to coherently control the $^{171}Yb^+$ qubit with microwave radiation has been demonstrated [4,13], and therefore is not treated here.

Two hyperfine levels, $|0\rangle \equiv |S_{1/2}, F=0\rangle$ and $|1\rangle \equiv |S_{1/2}, F=1\rangle$ of the $S_{1/2}$ ground state of $^{171}Yb^+$ serve as a qubit. In order to keep the experimental setup as simple as possible, it is desirable to achieve state preparation (as well as state selective detection) without adding more light sources to the setup. Therefore, we use the same optical transition near 369 nm from $|S_{1/2}, F=1\rangle$ to $|P_{1/2}, F=0\rangle$ that is used for laser cooling to also prepare and detect the qubit state. Optical pumping for state preparation from $|S_{1/2}, F=1\rangle$ into $|S_{1/2}, F=0\rangle$ is achieved by nonresonantly scattering light near 369 nm off the state $|P_{1/2}, F=1\rangle$. For laser cooling, optical pumping is not desired and is hindered by irradiating the ion simultaneously with radiation at 12.64 GHz driving the qubit transition from $|S_{1/2}, F=0\rangle$ to $|S_{1/2}, F=1\rangle$. Figure 4 shows the rate of detected photons near 369 nm as a function of time after turning off the microwave radiation, and thus depicts the optical pumping process into state $|0\rangle$.

The process just described serves simultaneously for state-selective detection as well as for state preparation, thus initializing the qubit for subsequent quantum logic operations: If, in step 3 of a quantum logic operation, the ion is in state $|0\rangle$, no scattered photons are detected; on the other hand, if the ion is in state $|1\rangle$, a number of photons is detected (see Fig. 4).

Even though the incident radiation at 369 nm is detuned by about 15 GHz from the resonance $|S_{1/2}, F=0\rangle \leftrightarrow |P_{1/2}, F=1\rangle$, this nonresonant scattering process leads to the depletion of the population in $|S_{1/2}, F=0\rangle$. As this process competes with state preparation, it diminishes the preparation efficiency. The optical pumping process has been investigated in detail (i) experimentally, and (ii), by solving the optical Bloch equations for this eight-level system in order to answer the following question: When using just one light field near 369 nm, and by including the possibility of switching its polarization and intensity, what is the optimal detection and preparation efficiency that can be obtained?

Figure 5(a) shows the experimentally determined preparation efficiency plotted against the angle between the polarization of the light field near 369 nm and the direction of the external magnetic field (with the detuning and intensity of the light field near 369 nm already optimized. The solid line

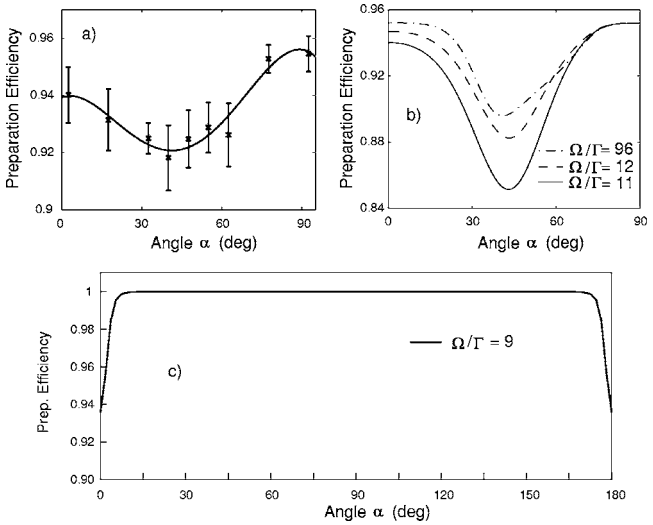

FIG. 5. The efficiency of the preparation of state $|0\rangle \equiv |S_{1/2}, F=0\rangle$ by optical pumping as a function of the angle α between the directions of light polarization and magnetic field, respectively. (a) Experiment. (b) Numerical simulation for different ratios of Rabi-frequency and spontaneous decay rate. (c) Simulation for resonant excitation of $|S_{1/2}, F=1\rangle \leftrightarrow |P_{1/2}, F=1\rangle$.

is meant to guide the eye. In Fig. 5(b), the computed preparation efficiency is plotted for three different light intensities (the Rabi frequency is given in units of the transition linewidth). Numerical simulations show that the maximal preparation efficiency achievable with a single light field near 369 nm is approximately 96.4%. The experimentally obtained maximal value is 95.5 (6)%.

Another approach to state preparation is resonant pumping of the transition $|S_{1/2}, F=1\rangle \leftrightarrow |P_{1/2}, F=1\rangle$ by a light field near 369 nm. The short-lived $|P_{1/2}, F=1\rangle$ state decays into both hyperfine sublevels of the $S_{1/2}$ ground state with a branching ratio of 2:1. Therefore, it takes only a few optical pumping cycles at a rate of 19.6 MHz to populate the $|S_{1/2}, F=1\rangle$ state with close to 100% efficiency. This is much faster than the nonresonant depletion process described above. Figure 5(c) shows the computed preparation efficiency close to 100%, which in addition, is nearly independent of the polarization angle.

$^{171}Yb^{+}$ possesses the simplest possible hyperfine structure of the electronic ground state $S_{1/2}$, and allows for choosing either a magnetic field insensitive qubit or qubit states whose energy separation depends on an applied magnetic field. The latter choice is suitable for experiments where (i) the coupling between internal and external ionic degrees of freedom (necessary for conditional quantum dynamics) relies on a state-dependent Zeeman force and (ii) ions are individually addressed in frequency space [11,14]. In a suitably modified ion trap, microwave radiation may be used *directly* for coherent manipulation of hyperfine qubits, thus eliminating all possible sources of error that are present when first imprinting frequency and phase information of microwaves onto laser radiation used for driving a Raman transition, and then illuminating ions with this light.

Financial support by the Deutsche Forschungsgemeinschaft, Science Foundation Ireland under Contract No. 03/IN3/I397, and by the European Union (QGates) is gratefully acknowledged.

[1] D. Leibfried *et al.*, Nature (London) **438**, 639 (2005).
[2] H. Häffner *et al.*, Nature (London) **438**, 643 (2005).
[3] B. B. Blinov *et al.*, Nature (London) **428**, 153 (2004).
[4] Ch. Wunderlich and Ch. Balzer, Adv. At., Mol., Opt. Phys. **49**, 293 (2003).
[5] Ch. Roos *et al.*, Phys. Rev. Lett. **83**, 4713 (1999).
[6] C. Langer *et al.*, Phys. Rev. Lett. **95**, 060502 (2005).
[7] The quoted number includes light fields employed for a generation of ions by photoionization: D. M. Lucas *et al.*, Phys. Rev. A **69**, 012711 (2004).
[8] N. Kjaergaard *et al.*, Appl. Phys. B: Lasers Opt. **71**, 207 (2000); S. Gulde *et al.*, *ibid.* **73**, 861 (2001).
[9] For instance, R. Blatt, H. Schnatz, and G. Werth, Phys. Rev. Lett. **48**, 1601 (1982); Chr. Tamm, D. Schnier, and A. Bauch, Appl. Phys. B: Lasers Opt. **60**, 19 (1995); P. Gill *et al.*, Phys. Rev. A **52**, R909 (1995). For a review, see P. T. H. Fisk, Rep. Prog. Phys. **60**, 761 (1997).
[10] For instance, J. J. Bollinger, W. M. Itano, D. J. Wineland, and D. J. Heinzen, Phys. Rev. A **54**, R4649 (1996); V. Giovannetti, S. Lloyd, and L. Maccone, Phys. Rev. Lett. **96**, 010401 (2006).
[11] F. Mintert and C. Wunderlich, Phys. Rev. Lett. **87**, 257904 (2001); C. Wunderlich, *Laser Physics at the Limit* (Springer, Heidelberg, 2001), p. 261; D. Mc Hugh and J. Twamley, Phys. Rev. A **71**, 012315 (2005).
[12] J. D. Prestage, G. J. Dick, and L. Maleki, J. Appl. Phys. **66**, 1013 (1989).
[13] Th. Hannemann, D. Reiss, C. Balzer, W. Neuhauser, P. E. Toschek, and C. Wunderlich, Phys. Rev. A **65**, 050303(R) (2002).
[14] This includes Penning traps, e.g., H. F. Powell, D. M. Segal, and R. C. Thompson, Phys. Rev. Lett. **89**, 093003 (2002).